Angewandte Chemie

Semiconductor Materials

DOI: 10.1002/ange.200502090

SrAlSiH: A Polyanionic Semiconductor Hydride**

*Thomas Björling, Dag Noréus, Kjell Jansson, Magnus Andersson, Ekaterina Leonova, Mattias Edén, Ulf Hålenius, and Ulrich Häussermann**

In 2000 Gingl et al. reported the synthesis and structural characterization of the novel compound $SrAl_2H_2$.[1] Contrary to the alanates $A_mAe_nAl_oH_{m+2n+3o}$ (A, Ae = alkali and alkaline-earth metal, respectively), this aluminum hydride is not fully hydrogenated and was described as a "Zintl phase hydride". It features a two-dimensional $[Al_2H_2]^{2-}$ polyanion in which the Al atoms are arranged as a puckered graphitic layer with three nearest neighbors. The vacant coordination site is taken by hydrogen and the compound appears to be charge-balanced (Figure 1 a). A structural entity with both Al–Al and Al–H bonds had not been observed before and is indeed remarkable.

Herein we report the synthesis of SrAlSiH, which is a further example of a polyanionic hydride that is structurally closely related to $SrAl_2H_2$. However, it displays striking differences in its properties. In contrast to metallic, thermally labile $SrAl_2H_2$, isoelectronic SrAlSiH is an air- and moisture-stable semiconductor with a thermal decomposition temperature that is among the highest known for hydride compounds. Additionally, SrAlSiH displays a peculiar electronic structure that suggests interesting transport properties. The combination of properties of SrAlSiH is unexpected for a

---

[*] Dr. K. Jansson, Dr. U. Häussermann
Inorganic Chemistry, Stockholm University
10691 Stockholm (Sweden)
Fax: (+46) 8-152-187
E-mail: ulrich@inorg.su.se

T. Björling, Prof. D. Noréus
Structural Chemistry, Stockholm University
10691 Stockholm (Sweden)

E. Leonova, Dr. M. Edén
Physical Chemistry, Stockholm University
10691 Stockholm (Sweden)

Prof. U. Hålenius
Department of Mineralogy, Swedish Museum of Natural History
10405 Stockholm (Sweden)

Dr. M. Andersson
Solid State Physics
IMIT, Royal Institute of Technology
KTH Electrum 229
16440 Kista (Sweden)

[**] This work was supported by the Swedish Research Council (VR) and the Henrik Granholm foundation. The European Union is also acknowledged for financial support through the European Project HYSTORY (contract number ENK6-CT-2002-00600). We thank Zheng Weng for instrumental NMR support.

Supporting information for this article is available on the WWW under http://www.angewandte.org or from the author.

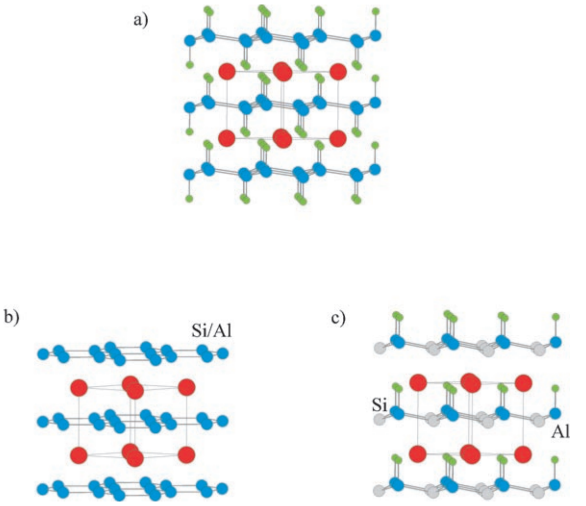

Figure 1. Crystal structures of $SrAl_2H_2$ (a), SrAlSi (b), and SrAlSiH (c) viewed along [110]. Red, blue, gray, and green circles denote Sr, Al (Al/Si), Si, and H atoms, respectively.

hydride and prompts an important issue: Polyanionic ("Zintl phase") hydrides provide novel coordination environments for H atoms and possess a huge compositional potential that is virtually unexplored. If physical properties inherent to hydrides and Zintl phases can be combined in these materials unexpected prospects are opened, thereby extending hydride materials' research beyond the traditional quest for hydrogen storage materials.[2]

SrAlSiH is obtained by hydrogenation of the alloy SrAlSi. This alloy is part of the solid solution $SrAl_{2-x}Si_x$ ($0.6 < x < 1.2$), which crystallizes in the hexagonal AlB_2 structure.[3] It is assumed that the Al and Si atoms in SrAlSi are more or less randomly distributed on the AlB_2 majority site, defining graphitic nets (Figure 1b). At a hydrogen pressure of 50 bar complete hydrogenation is typically obtained at temperatures between 600 and 700 °C and reaction times of 48 h. The refined lattice parameters of the final product are $a = 4.2139(3)$ and $c = 4.9550(6)$ Å. The c lattice parameter of the hydrogenated product is 5% larger than that of the starting material SrAlSi ($a = 4.2367(7)$, $c = 4.7442(9)$ Å), whereas the a lattice parameters are very similar. SrAlSiH possesses a gray and is air and moisture stable. This is remarkable in view of the sensitivity of other main group metal hydrides containing aluminium (e.g., alanates, $SrAl_2H_2$), which rapidly decompose when exposed to air and moisture. Another interesting observation is that when SrAlSi is employed in a compacted form for hydrogenation reactions (e.g. as a pellet or ingot), the shape of the starting material sample is completely preserved in the reaction product. In particular, single crystals of SrAlSi are transformed into identically shaped crystals of the hydrogenated product. Again, this is a remarkable feature because solid-state hydrogenations typically yield finely powdered products.

The structure of SrAlSiH (Figure 1c) was determined unambiguously by the refinement of neutron powder diffraction data of a deuterated sample (SrAlSiD) and by solid-state NMR investigations. It displays slightly puckered hexagon nets in which Si and Al atoms are arranged strictly alternately. H is exclusively attached to Al, and the Al–D distance in the deuteride is 1.77 Å. These puckered nets are stacked on top of each other, with the same orientation, and sandwich Sr atoms. Thus, compared with the starting material SrAlSi, the hydride experiences only small structural changes, which explains why single crystals of SrAlSi undergo hydrogenation into SrSiAlH without deterioration. In particular, the planar hexagon nets in SrAlSi become puckered in the hydride, and at the same time the interatomic distances within the nets increase from 2.46 to 2.50 Å. This leaves the a lattice parameter of both compounds about the same, whereas the c parameter is increased in the hydride.

Figure 2 shows magic-angle spinning (MAS) ^{27}Al (a), ^{29}Si (b), and ^{2}H NMR spectra (c) of a powder of SrSiAlD. Each spectrum is characteristic of a single site, as expected for a perfectly ordered structure consisting of hexagon nets of alternating Al and Si atoms, with ^{2}H exclusively attached to Al. As this sample displays comparatively long T_1 relaxation times for each of the nuclei involved, the absence of addi-

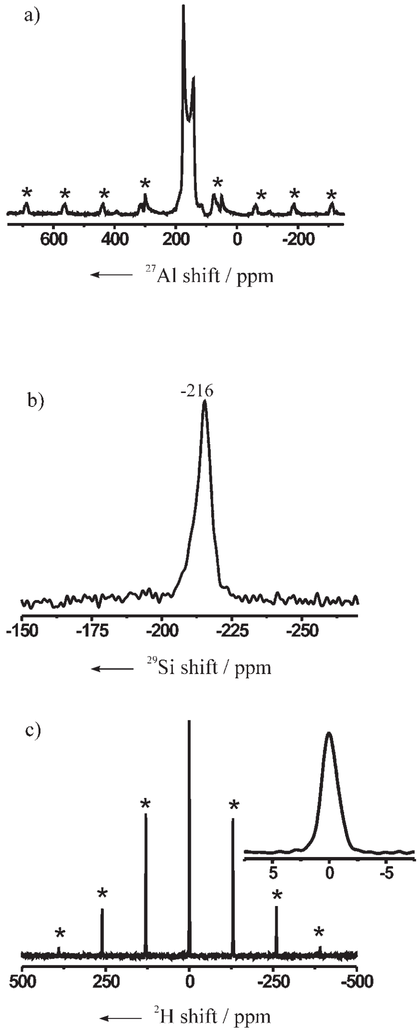

Figure 2. Magic-angle-spinning NMR spectra of SrSiAlD at 9.4 T. a) ^{27}Al spectrum recorded at 13.0 kHz spinning frequency. Asterisks indicate spinning sidebands. b) ^{29}Si spectrum at 8.0 kHz spinning frequency. c) ^{2}H spectrum at 8.0 kHz. The inset spectrum is a zoom around the centerband region.

tional spectral components was verified by saturation-recovery experiments. The ^{27}Al NMR spectrum displays a characteristic second-order powder line-shape of a well crystalline compound.[4] In conjunction with 3QMAS data[5] and numerical simulations (not shown), we estimated the isotropic chemical shift and quadrupolar parameters as follows: $\delta_{\text{iso}} = 185.5 \pm 1.5$ ppm, $C_Q = e^2 q Q/h = 7.5 \pm 0.2$ MHz, and $\eta < 0.1$.[6] As expected from the proposed structure, the local symmetry around Al is associated with an axially symmetric electric field gradient tensor. The ^{2}H spectrum corresponds to a main resonance at $\delta = 0$ ppm flanked by a set of spinning sidebands generated from the quadrupolar interaction and associated with a small quadrupolar coupling constant, $C_Q = 26 \pm 3$ kHz.

The structure of SrAlSiH is very similar to that of $SrAl_2H_2$ (see Figure 1): half of the Al–H entities in the 2D polyanionic layer of $SrAl_2H_2$ are replaced by isoelectronic Si. This replacement occurs in a completely ordered way, that is, each Si atom is surrounded by three Al–H entities and vice versa. The center of inversion present in $SrAl_2H_2$ is lost in SrSiAlH and the space-group symmetry is reduced to $P3m1$. The interatomic distances and angles of $SrAl_2H_2$ and SrAlSiH are given as Supporting Information. The most conspicuous difference between the two structures is that the Sr atom in SrAlSiH is only coordinated by three H atoms. The Sr–H distance in SrAlSiH is considerably smaller than in $SrAl_2H_2$ (2.48 vs 2.65 Å) and the Al–H distance significantly larger (1.77 vs. 1.71 Å). Both compounds possess electron-precise polyanions—$[Al_2H_2]^{2-}$ and $[AlHSi]^{2-}$—with structures in accordance with the Zintl concept.

Despite their great structural similarity the thermal behavior of $SrAl_2H_2$ and SrAlSiH is strikingly different. Figure 3 displays heat-effect curves for both compounds at atmospheric pressure. Hydrogen desorption starts at 300 °C for $SrAl_2H_2$, whereas SrAlSiH only starts to decompose at temperatures above 600 °C. Higher decomposition temperatures are only known for some saline alkali and alkaline-earth metal hydrides.[7] Furthermore, hydrogen release of $SrAl_2H_2$ produces a mixture of the intermetallic compounds $SrAl_2$ and $SrAl_4$, whereas in the case of SrAlSiH the starting material SrAlSi is quantitatively regained. This means that although the Al–H distance in SrAlSiH is longer than in $SrAl_2H_2$, hydrogen is more tightly bound in SrAlSiH. This is easily explained by the higher positively charged environment that H experiences in SrAlSiH. Firstly, Al—to which H is attached—is positively polarized by the surrounding Si atoms in the polyanion, and secondly the Sr–H distance in SrAlSiH is considerably smaller. As a matter of fact, the Sr–H distance in SrAlSiH corresponds very well to the smallest Sr–H distances in saline SrH_2 (2.43–2.48 Å).[8]

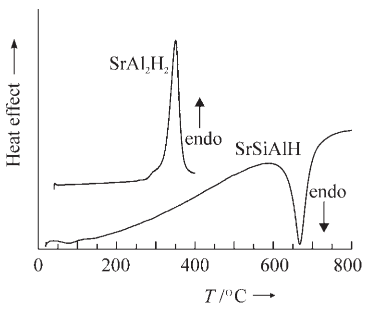

Figure 3. Heat-effect curves for $SrAl_2H_2$ (DSC) and SrAlSiH (DTA).

Figure 4 compares the electronic density of states (DOS) of $SrAl_2H_2$ and SrAlSiH in their computationally relaxed equilibrium structures. The Fermi level for $SrAl_2H_2$ is situated at a pseudo gap. The metallic behavior of this compound is due to Al p bands crossing the Fermi level. In contrast, a real bandgap of about 0.65 eV is opened at the Fermi level for SrAlSiH and the compound is a semiconductor. The contribution of Sr atoms to the occupied states is rather low for both compounds, but rises sharply above the Fermi level (see Supporting Information). This is a typical feature of polar intermetallic and Zintl phases. The contribution of H is mainly into the intermediate energy regions of the DOS (between −6.5 and −2 eV), which are the parts where Al s and p bands mix strongly. The DOS of SrAlSiH is characterized by a pronounced singularity below the Fermi level. As can be seen in the band structure (Figure 4c), this singularity originates from a flat band corresponding to the Si p_z (lone pair) orbitals. These orbitals are virtually isolated in SrAlSiH and the arising band displays a very small dispersion. As a consequence, this compound attains a peculiar electronic structure in which a narrow bandgap is combined with a flat band exactly below the Fermi level.

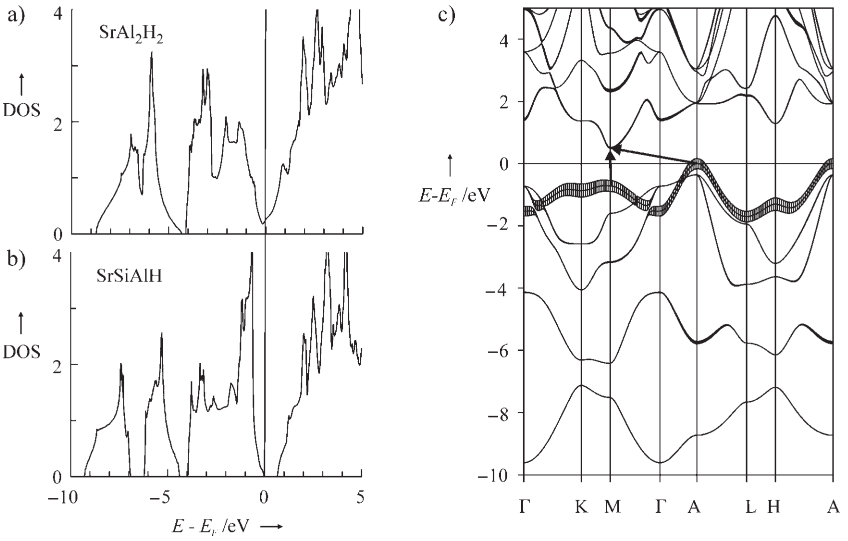

Figure 4. Electronic density of states, DOS (states $eV^{-1} Z^{-1}$), for $SrAl_2H_2$ (a) and SrAlSiH (b). The Fermi level is indicated by a vertical line. c) Band structure of SrAlSiH. The Si p_z orbital contribution is shown as broad-band representation. The lowest energy transition A→M, which is indirect, and the direct transition with lowest energy are indicated as arrows.

According to the calculated band structure the bandgap is of indirect nature; the valence band maximum is located at Γ and the conduction band minimum at M. Optical absorption spectra obtained from diffuse reflectance measurements confirmed the presence of the bandgap. The experimental value of 0.63 eV is, coincidentally, in close agreement with the calculated one. The room-temperature resistivity of SrAlSiH is about 110 Ω cm, which can be compared to the intrinsic room-temperature resistivity of Ge (46 Ω cm) with a bandgap of 0.73 eV. The thermopower of SrAlSiH is around $-90\,\mu V K^{-1}$ at room temperature, and the negative sign of the Seebeck coefficient implies that electrons are the charge carriers in this material (see Supporting Information for further details).

In conclusion, we have reported on the novel semiconductor hydride SrAlSiH. Several aspects make this compound remarkable: 1) SrAlSiH is, after $SrAl_2H_2$, the second example of a "Zintl phase hydride" where H is part of a polyanion. The two-dimensional polyanion of SrAlSiH is composed of isolectronic, three-bonded $[Al{-}H]^-$ and Si^- entities and is charge balanced by Sr^{2+}. 2) SrAlSiH is a semiconductor with an indirect bandgap of about 0.65 eV. Metal hydrides with narrow bandgap (0.2–1.2 eV) semiconductor properties are unprecedented; fully hydrogenated main group metal systems are typically insulators. The wide homogeneity range of underlying AlB_2-type $SrAl_{2-x}Si_x$ ($0.6 < x < 1.2$) may allow triggering of a transition to a metallic $SrAl_{2-x}Si_xH_{2-x}$ for low values of x. In this case, the Fermi level would cut the singularity in the DOS which may give rise to superconductivity. On the other hand, for $x > 1$ a widening of the bandgap is expected. 3) The NMR investigation of SrAlSiD has provided the first ^{27}Al and ^{29}Si data for a structure involving direct Al–Si contacts and where spectral resolution is not limited by fast T_2-relaxation, which is observed in metallic compounds because of the conducting electrons.[9] The ^{29}Si chemical shift ($\delta_{Si} = -216$ ppm) implies large diamagnetic contributions due to the localized negative charge of a lone electron pair at Si. This shift is somewhat more shielded than observed for the ^{29}Si site in antifluorite-type Mg_2Si ($\delta_{Si} = -177$ ppm), where formally Si^{4-} is cubically surrounded by eight strongly polarizing Mg^{2+} ions.[10] The large paramagnetic contribution to the isotropic ^{27}Al chemical shift ($\delta_{Al} = 185.5$ ppm) arises from a high degree of charge asymmetry at the Al nucleus due to bonding to two different ligands, Si and D (also reflected in the relatively high quadrupolar coupling constant).[11] 4) Al and Si are strictly ordered in SrAlSiH. This is in contrast to the starting material SrAlSi, where Al and Si are distributed more or less randomly. It is known that conventional (disordered) SrAlSi is a superconductor with a T_c of 5.1 K.[3] However, the nature of the superconducting properties remains unclear.[12] Hydrogen desorption of SrAlSiH provides an elegant way to obtain ordered SrAlSi. The study of the ordered material could provide some deeper understanding of the superconducting properties of SrAlSi.

Experimental Section

Synthesis: All steps of the synthesis and sample preparation for diffraction experiments were carried out under dry argon. The starting materials $SrAl_2$ and SrSiAl were prepared by arc-melting stoichiometric mixtures of the pure elements. For hydrogenation, the starting materials were loaded in corundum crucibles, which were placed in stainless steel autoclaves. Reactions were carried out at 50–60 bar hydrogen pressure and temperatures of 200 °C and 700 °C for $SrAl_2$ and SrAlSi, respectively. SrAlSiD was prepared analogously. Starting materials and hydrides were characterized by Guinier powder patterns (Cu Kα_1; Si standard) and EDX (energy-disperse X-ray) analysis in a JEOL 820 scanning electron microscope. SrAlSiH can be exposed to air and moisture without decomposition.

Structural characterization: Lattice constants of SrAlSi, SrAlSiH, and SrAlSiD were obtained from least-squares refinement of measured and indexed lines of the corresponding Guinier powder diffractograms.[13] Atomic positions of SrAlSiD were determined from a Rietveld refinement of neutron powder diffraction data[14] collected at the Studsvik Neutron Research Laboratory, Sweden (room temperature, $\lambda = 1.47$ Å, data resolution $\Delta d/d = 2 \times 10^{-3}$). SrAlSiD: space group $P3m1$ (no. 156); cell parameters (X-rays): $a = 4.2113(3)$, $c = 4.9518(5)$ Å, $V = 76.05$ Å^3, $Z = 1$; $R_B = 1.87\,\%$, $R_P = 9.49\,\%$, $R_{wp} = 9.44\,\%$, $\chi^2 = 1.44$ for 85 reflections (positional parameters are provided as Supporting Information).

NMR spectroscopy: MAS NMR experiments were carried out at room temperature on a Varian/Chemagnetics Infinity-400 spectrometer operating at 9.4 T, giving the Larmor frequencies −61.43, −104.28, and 79.50 MHz and for ^2H (spin 1), ^{27}Al (spin 5/2), and ^{29}Si (spin 1/2), respectively. Powders of SrSiAlD (99 % enriched with respect to ^2H) were filled in zirconia rotors of outer diameters 3.2, 4, and 6 mm, and spun at 8.0 (for ^2H acquisitions), 13.0 (^{27}Al), and 8.0 kHz (^{29}Si), respectively. 48 ^2H signal transients were recorded with 90° pulses (76 kHz nutation frequency) and 120 s relaxation delays. The ^{29}Si spectrum was recorded using 30° pulses and 188 accumulated transients with 600 s relaxation delays. ^{27}Al acquisitions resulted from 840 transients, 60 s relaxation delays, and 11° pulses (86 kHz nutation frequency, measured with respect to Al^{3+}(aq)). No additional line-broadening was applied in the spectral processing. Chemical shifts are reported in deshielding (δ) units of ppm, referenced externally to D_2O (^2H), Al^{3+}(aq) (^{27}Al), and TMS (^{29}Si).

Thermal investigations: The thermal behavior of powdered samples of $SrAl_2H_2$ and SrAlSiH was investigated by differential thermal analysis (DTA-TG, Setaram Labsys 1600) and differential scanning calorimetry (Perkin Elmer DSC 7), respectively. $SrAl_2H_2$ was placed in a steel container, which was sealed with gold foil to prevent exposure to air and moisture, and the temperature was raised from 40 to 400 °C. SrAlSiH was placed in an open corundum crucible and the temperature was raised from 40 to 800 °C. Both experiments were performed under a flow of dry argon and with a temperature-increase rate of $5\,K\,min^{-1}$.

Diffuse reflectance measurements: Optical diffuse reflectance measurements were made on finely ground samples of SrAlSiH and SrAlSiD at room temperature. The spectrum was recorded in the region 3200–10 500 cm^{-1} with a Bruker Equinox 55 FT-IR spectrometer equipped with a diffuse reflectance accessory (Harrick). The measurement of diffuse reflectivity can be used to determine bandgaps. For this, absorption data (α/S) were extracted from the reflectance data by using the Kubelka–Munk function.[15]

Resistivity and thermopower measurements: Resistivity measurements were performed using a four-point in-line contact arrangement on a $2 \times 3.3 \times 6$ mm^3 bar of SrAlSiH. This bar was obtained by polishing an ingot of SrAlSi and subsequent hydrogenation. The thermoelectric voltage, U, was measured for different temperature gradients ΔT between two sides of the bar. A straight line was fitted to $U(\Delta T)$, which has the slope $dU/d(\Delta T) = S_w - S_s$, where S_s is the thermopower of the sample and S_w is the thermopower of the connecting wires.

Electronic structure calculations: Total energy calculations for $SrAl_2H_2$ and SrAlSiH were performed in the framework of the frozen core all-electron Projected Augmented Wave (PAW) method,[16] as implemented in the program VASP.[17] The energy cut-off was set to 500 eV. Exchange and correlation effects were treated by the generalized gradient approximation (GGA), usually referred to as

PW91.[18] The integration over the Brillouin zone was done on special *k*-points determined according to the Monkhorst–Pack scheme.[19] Total energies were converged to at least 1 meV per atom. Structural parameters were relaxed until forces had converged to less than 0.01 eV Å^{-1}.

Received: June 16, 2005
Revised: August 31, 2005

Keywords: aluminum · hydrides · NMR spectroscopy · semiconductors · zintl phases

---

[1] F. Gingl, T. Vogt, E. Akiba, *J. Alloys Compd.* **2000**, *306*, 127.
[2] A. M. Seayad, D. M. Antonelli, *Adv. Mater.* **2004**, *16*, 765.
[3] B. Lorenz, J. Lenzi, J. Cmaidalka, R. L. Meng, Y. Y. Sun, Y. Y. Xue, C. W. Chu, *Phys. C* **2002**, *383*, 191.
[4] K. J. D. McKenzie, M. E. Smith, *Multinuclear Solid-State NMR of Inorganic Materials* (Pergamon Materials Series 6), Elsevier, Amsterdam, **2002**.
[5] L. Frydman, J. S. Harwood, *J. Am. Chem. Soc.* **1995**, *117*, 5367.
[6] The asymmetry parameter of the electric-field gradient tensor is defined as $\eta = (V_{yy} - V_{xx})/V_{zz}$ $(0 \leq \eta \leq 1)$, with the principal values, V_{ii}, ordered according to $|V_{yy}| \leq |V_{xx}| \leq |V_{zz}|$.
[7] W. Grochala, P. P. Edwards, *Chem. Rev.* **2004**, *104*, 1283.
[8] N. E. Brese, M. O'Keeffe, R. B. von Dreele, *J. Solid State Chem.* **1990**, *88*, 571.
[9] However, as the ^{29}Si peak (Figure 2b) is rather broad and slightly asymmetric, we believe its width is primarily dictated by unresolved splittings from scalar couplings to its ^{27}Al neighbors. Broadening may also stem from "residual" ^{27}Al–^{29}Si dipolar couplings, unaveraged by MAS due to the ^{27}Al quadrupolar interaction [R. K. Harris, A. Olivieri, *Prog. Nucl. Magn. Reson. Spectrosc.* **1992**, *24*, 435], as observed even across Si–O–Al linkages in minerals at low magnetic fields [J. S. Hartman, B. L. Sheriff, *J. Phys. Chem.* **1991**, *95*, 7575].
[10] E. Ratai, M. P. Augustine, S. M. Kauzlarich, *J. Phys. Chem. B* **2003**, *107*, 12573.
[11] For comparison, the chemical shifts of the tetrahedral ^{27}Al site in the III–V semiconductors AlP and AlAs are $\delta = 142$ and 130 ppm, respectively [O. H. Han, H. K. C. Timken, E. Oldfield, *J. Chem. Phys.* **1988**, *89*, 6046].
[12] I. I. Mazin, D. A. Papaconstantopoulos, *Phys. Rev. B* **2004**, *69*, 180512.
[13] P.-E. Werner, *Ark. Kemi* **1969**, *31*, 513.
[14] J. Rodriguez-Carvajal, *FULLPROF: A Program for Rietveld Refinement and Pattern Matching Analysis*, Abstracts of the Satellite Meeting on Powder Diffraction of the XV Congress of the IUCr, Toulouse, France, **1990**, p. 127.
[15] G. Kotiim, *Reflectance Spectroscopy*, Springer, New York, **1969**.
[16] a) P. E. Blöchl, *Phys. Rev. B* **1994**, *50*, 17953; b) G. Kresse, J. Joubert, *Phys. Rev. B* **1999**, *59*, 1758.
[17] a) G. Kresse, J. Hafner, *Phys. Rev. B* **1993**, *47*, 558; b) G. Kresse, J. Furthmüller, *Phys. Rev. B* **1996**, *54*, 11169.
[18] J. P. Perdew, Y. Wang, *Phys. Rev. B* **1992**, *45*, 13244.
[19] H. J. Monkhorst, J. D. Pack, *Phys. Rev. B* **1972**, *13*, 5188.